NATIONAL AERONAUTICS AND SPACE ADMINISTRATION

Technical Memorandum No. 33-270

Pyrotechnic Shock Analysis and Testing Methods

Alan R. Hoffman

James E. Randolph

jpl

JET PROPULSION LABORATORY

CALIFORNIA INSTITUTE OF TECHNOLOGY

PASADENA, CALIFORNIA

February 15, 1966

NATIONAL AERONAUTICS AND SPACE ADMINISTRATION

Technical Memorandum No. 33-270

Pyrotechnic Shock Analysis and Testing Methods

Alan R. Hoffman
James E. Randolph

W. S. Shipley, Manager
Environmental Requirements Section

JET PROPULSION LABORATORY
CALIFORNIA INSTITUTE OF TECHNOLOGY
PASADENA, CALIFORNIA

February 15, 1966

Prepared Under Contract No. NAS 7-100
National Aeronautics & Space Administration

CONTENTS

TABLES

FIGURES

FIGURES (Cont'd)

ABSTRACT

Explosive separation devices employed during the launch phase and space flight generate a shock environment that could have a deleterious effect on the spacecraft hardware. The interpretation and simulation of these shocks in ground tests are necessary to insure equipment integrity during this phase.

This Report presents a detailed analysis of certain pyrotechnic shocks. The data used are from the *Ranger Block III* and *Mariner-Mars* test programs. Shock spectra form the basis of correlation between similar shocks of various spacecraft and assembly testing. Comparisons of shock data using statistical methods are also included. Since a wealth of shock data was available, the statistical analysis is significant.

The results indicate the necessity for a system-level pyrotechnic test program if the environment is to be properly simulated.

I. INTRODUCTION

Explosive separation devices are characterized by relatively short-duration shocks of high magnitude. The separation events near the payload area of a vehicle may include shroud separation, electrical separation, and mechanical separation. Also, pyrotechnic devices are used to deploy such items as solar panels or scientific instruments. The pyrotechnics generate shock pulses that could have a deleterious effect on the spacecraft operability.

This Report will not consider transients associated with booster staging or engine start-shutdown or those associated with lunar or planetary impact. Only shock transients related to pyrotechnics near the payload area will be discussed.

The data used for the majority of this Report come from the *Ranger* test program. The remainder are drawn from the *Mariner-Mars* test program. Both of these programs were conducted at the Jet Propulsion Laboratory (JPL), Pasadena, California, during 1963–1965.

Ranger was an unmanned lunar probe 9.25-ft high (launch configuration) and weighed approximately 804 lb. *Mariner IV (Mariner-Mars)* flew by Mars July 14, 1965, on a scientific and photographic mission. Its weight was approximately 575 lb.

The launch vehicle for *Ranger* was the *Atlas/Agena B;* for *Mariner-Mars*, it was the *Atlas/Agena D*.

Figures 1, 2, and 3 show three typical pinpullers used for the *Ranger* program. The electrical separation pinpuller (Fig. 1) drives pins against the brackets. The spin collar releases the connector and a spring pulls the lower connector away from the spacecraft. The mechanical separation pinpuller (Fig. 2) retracts a pin, and spring loading separates the spacecraft from the launch vehicle. The shroud separation pinpullers operate in an identical manner. The solar-panel pinpullers (Fig. 3) release the panels after launch by retracting a pin. The panels are slowly extended by an actuator. Rubber grommets were inserted between the solar-panel pinpuller and the spacecraft structure to reduce responses at the higher frequencies. Figure 4 shows the *Ranger* test configuration. Similar pinpullers were used on *Mariner* for solar-panel and scan-platform deployment, but *V* bands affected both shroud and mechanical separation.

The number of pinpullers used on *Ranger* and *Mariner-Mars* is given in Table 1. For reliability, two squibs are mounted in the pinpullers, either one of which could cause actuation. Also, for reliability, separate circuitry for firing of each squib was used.

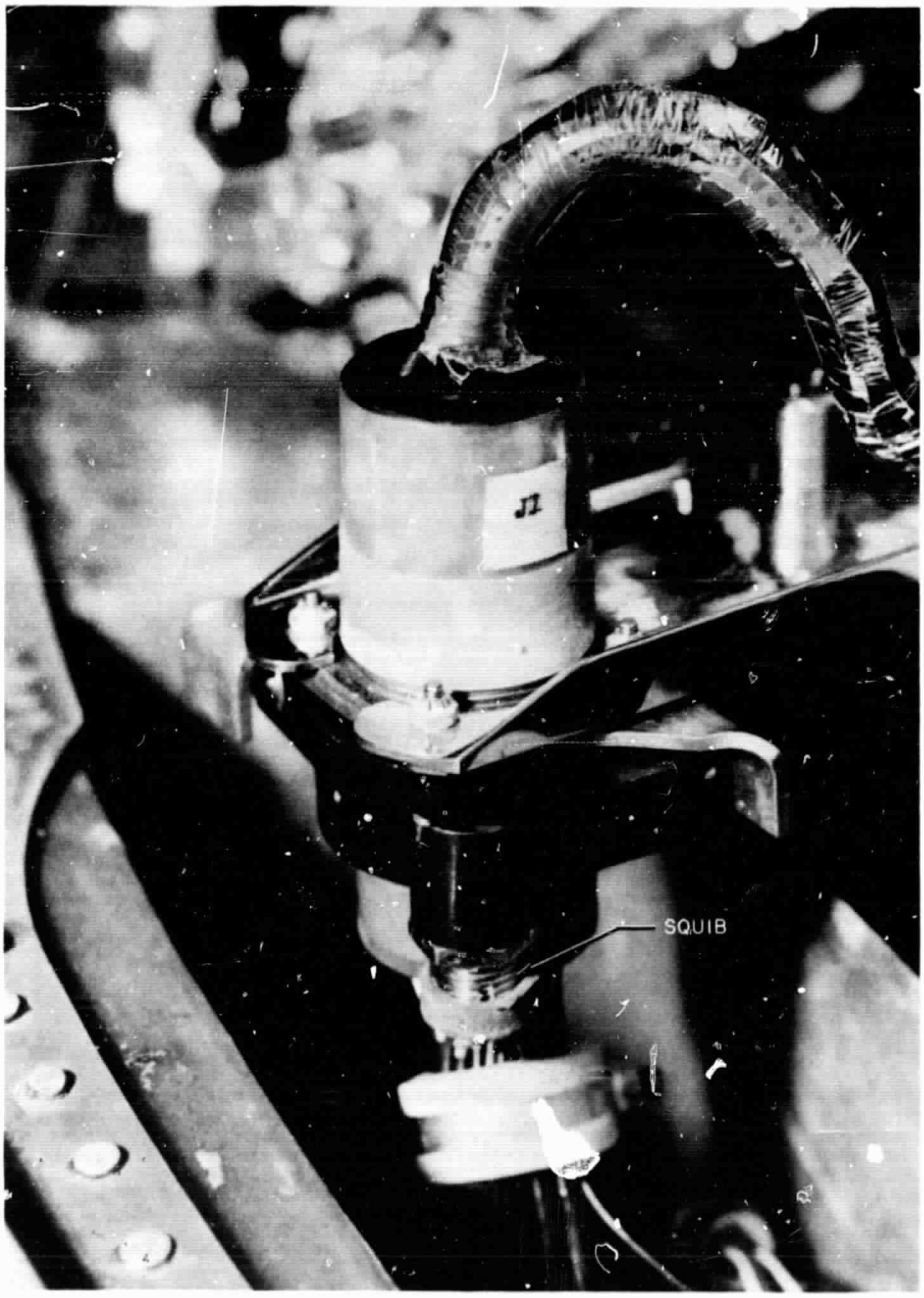

Fig. 1. ***Ranger*** **electrical-separation pyrotechnic**

Table 1. Number of pinpullers for *Ranger* and *Mariner-Mars*

Pyrotechnic events	*Ranger*	*Mariner-Mars*
Shroud separation	3	V band
Electrical separation	2	(not pyrotechnically separated)
Mechanical separation	3	V band
Solar-panel deploy	4	8
Scan platform	—	1

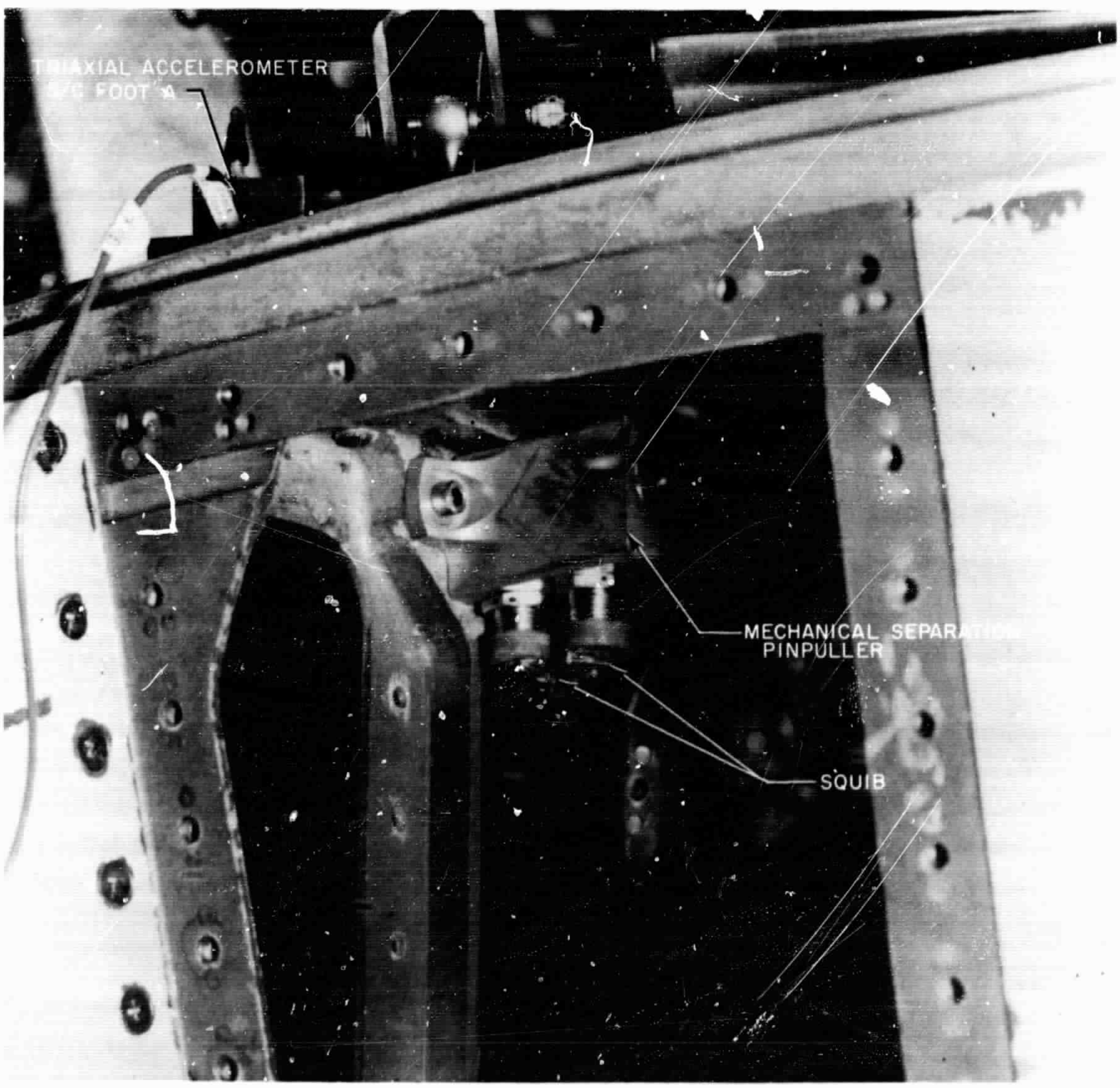

Fig. 2. *Ranger* mechanical-separation pinpuller

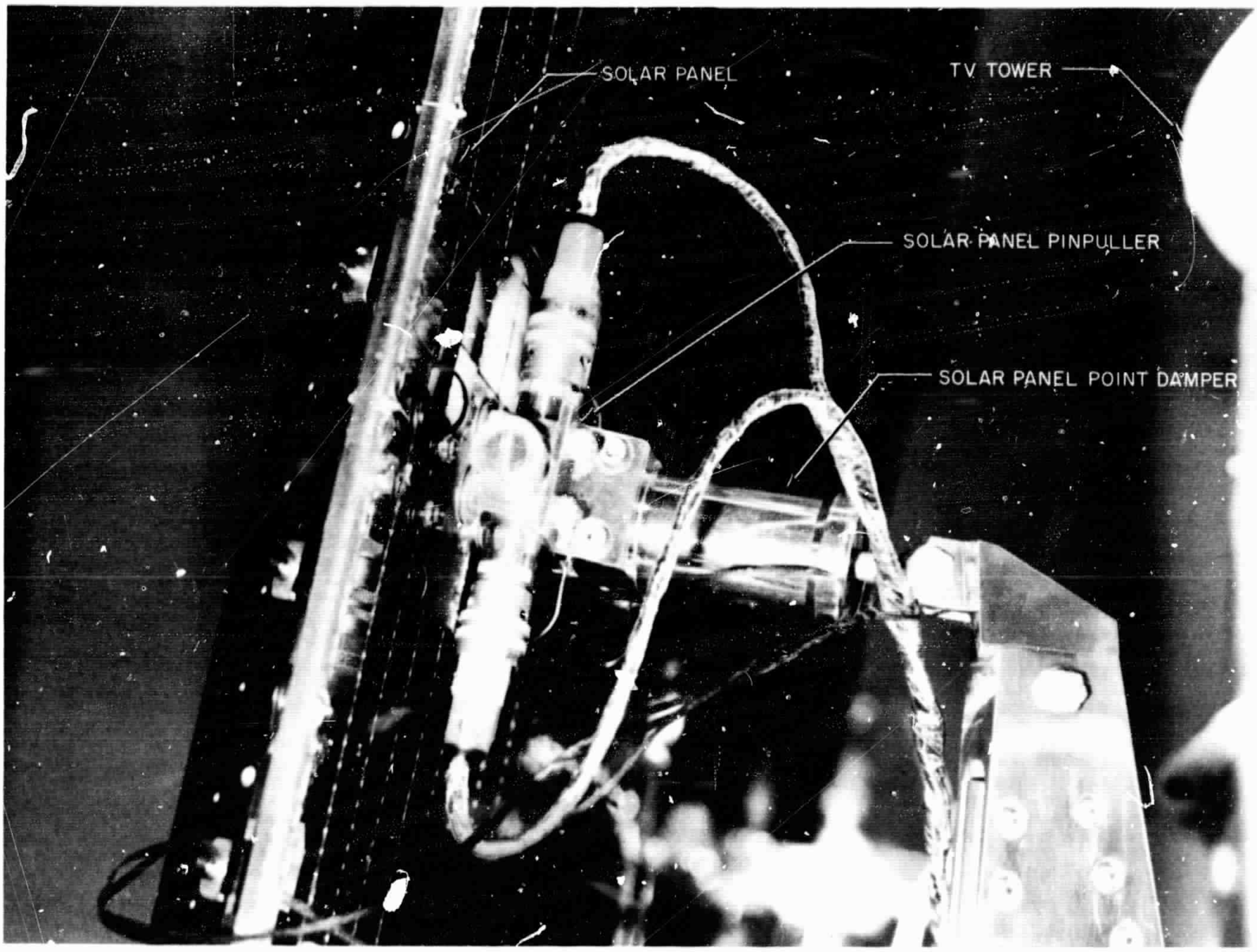

Fig. 3. *Ranger* solar-panel pinpuller

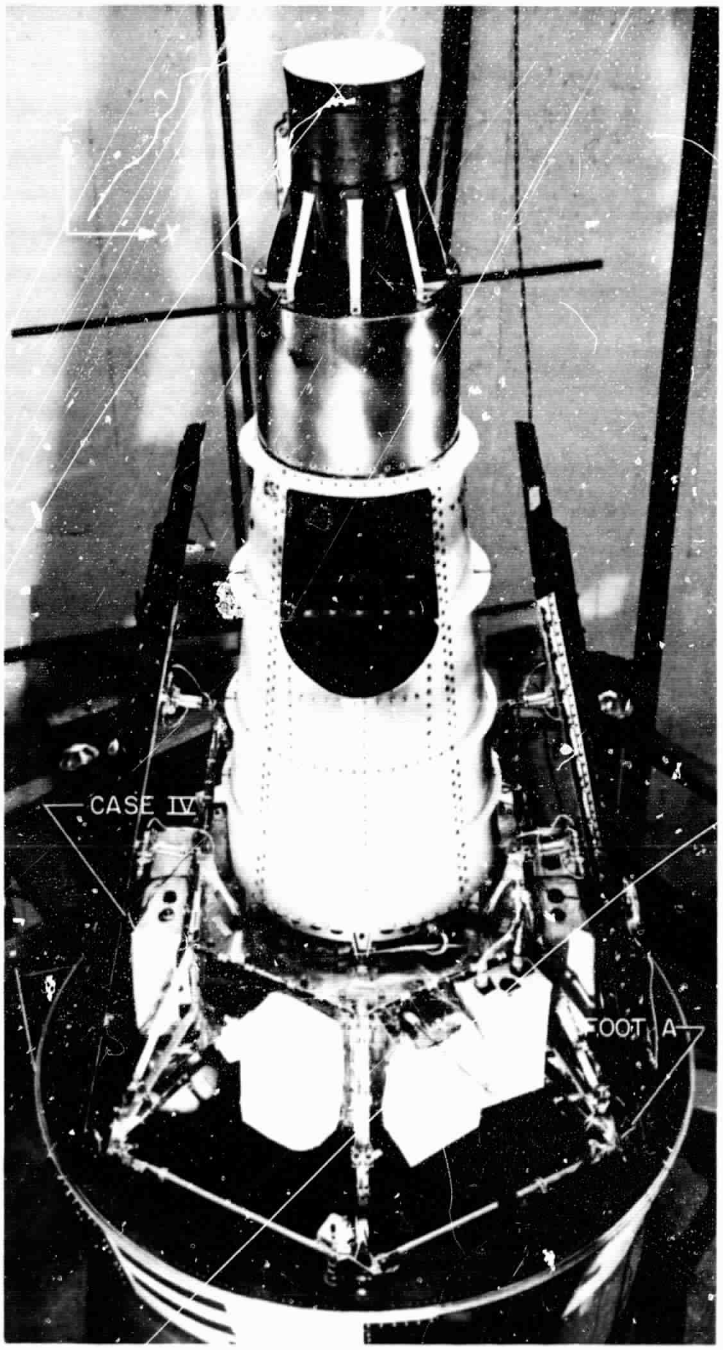

Fig. 4. *Ranger* pyrotechnic test configuration

II. TESTING METHODS

Hardware integrity and operability in the environment were demonstrated on the assembly level and system level prior to the commitment to flight.

The assembly shock test requirement for the type approval (TA) assembly consisted of a terminal peak sawtooth 0.5 to 1.5 msec in duration and 100 g's or 200 g's in magnitude depending on installation. The test was repeated five times in each orthogonal axis for a total of fifteen shocks.

The shock test requirements were based upon experience obtained from earlier programs. Since the present-day shock machines cannot excite the high frequencies associated with pyrotechnic devices without excessive test response at the low frequencies, a tradeoff in test duration had to be made. In other words, the shock from a shock machine does not simulate the shock from the use of pyrotechnics. This point will be considered in detail later in this Report.

Fig. 5. Shock machine for assembly level testing

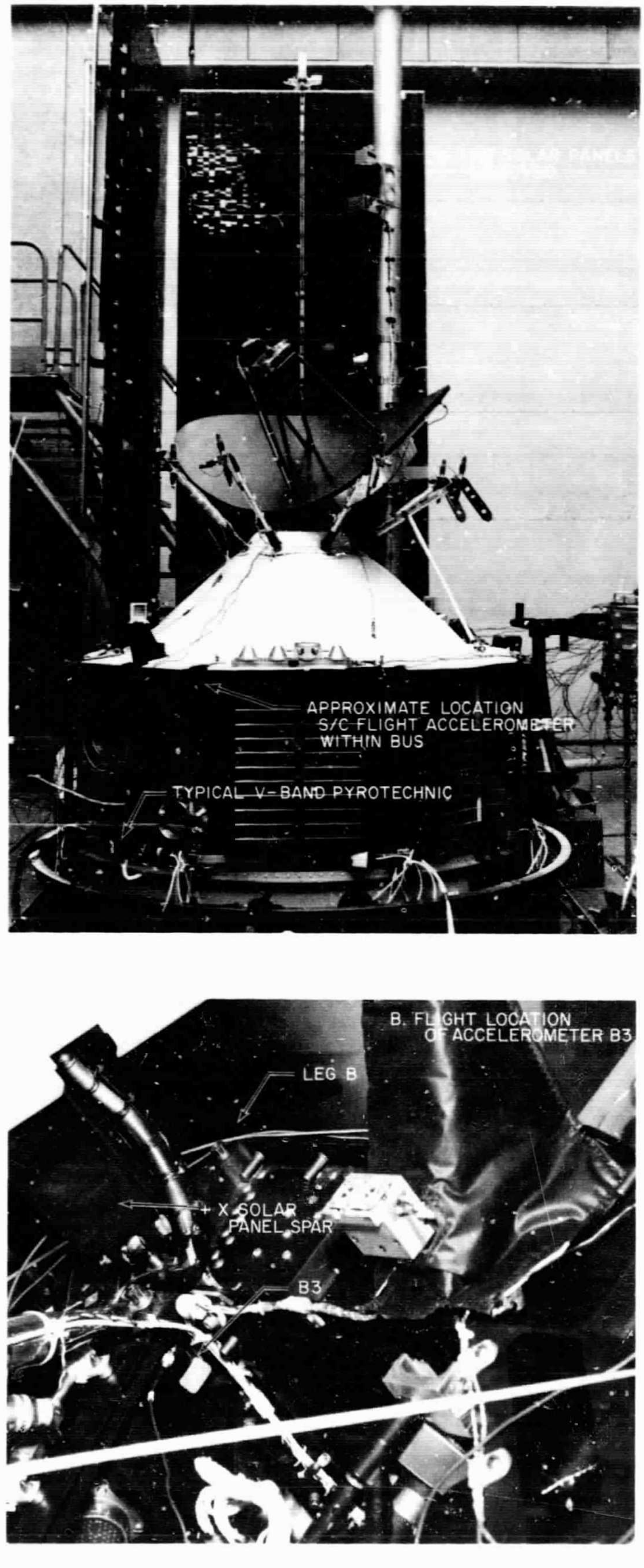

Fig. 6. *Mariner-Mars* spacecraft

The shock machine shown in Fig. 5 was the one used for the majority of the *Ranger* and *Mariner-Mars* testing.

Ranger had no failures reported during TA testing. *Mariner-Mars* had three failures in 116 tests, all latching-relay malfunctions.

To demonstrate the proper operation of the spacecraft in the environments, especially the high-frequency transients not covered by the TA tests, a series of tests using flight-type pyrotechnics was performed at the spacecraft level.

For system level tests, the *Ranger* proof test model (PTM) was mounted on the adapter and the forward equipment rack of the launch vehicle. The test configuration for *Ranger* is shown in Fig. 4. The pinpullers actuated were the electrical-separation, mechanical-separation, and solar-panel ones. These were chosen because (1) each of these transmits loading through different paths, and (2) the magnitude of the transients associated with these pinpullers is significant. The shroud-separation pinpullers were not used because the loading path and transient magnitude are similar to the mechanical-separation pinpullers, i.e., are located in close proximity. The most severe shocks occurred during mechanical separation.

A typical *Mariner-Mars* test configuration is shown in Fig. 6. The shock test consisted of the actual firing of the pyrotechnic devices on board the spacecraft. The following tests were performed: (1) shroud *V*-band release, (2) spacecraft *V*-band release, (3) solar-panel release, and (4) science-platform release. The most severe shocks occurred during the spacecraft *V*-band release. Low-frequency ring-out due to the release of the stored energy in the deformed structure was detected.

For the *Ranger* PTM, the electrical separation was performed twice, the mechanical separation five times, and solar-panel deployment six times. Transient simulation was the primary objective during the electrical separation and mechanical separation.

A special test, in which the pyrotechnically actuated midcourse motor valves were fired, demonstrated that there were not significant responses at the other parts of the spacecraft.

Each *Ranger* spacecraft had the solar-panel pinpullers fired at least once. The primary purpose was to verify circuitry with live squibs installed. The transient simulation was a secondary consideration.

Environmental data were measured on all these tests. The frequency response of typical accelerometers has been checked. The results are shown in Table 2. A description of the special test performed to verify the response of accelerometers, used in the test programs, to transient excitation is given in the Appendix.

Table 2. Typical accelerometer characteristics

Accelerometer	Manufacturer's specifications			Frequency response from special transient test[c]	*Ranger* spacecraft location
	Frequency response[a]	Accelerometer mounted resonance frequency[b] (kc)	Amplitude linearity		
Endevco 2225	±10% 2 cps–15 kc	80	±2% 0–20,000 g	+0% −8% 200 cps–10 kc	Case IV[e]
Columbia 514[d]	± 5% 2 cps–5 kc	30	±1%	+6% −0% 200 cps–8 kc	Foot A
				+46% −0% 8 kc–10 kc	
Endevco 2213	± 5% 2 cps–7 kc	35	±2% 0–500 g	+5% −1% 100 cps–10 kc	Case I, Leg A
Endevco 2217	± 5% 2 cps–6 kc	30	±2% 0–300 g	+0% −3% 200 cps–10 kc	Flight position (*Ranger* and *Mariner-Mars*)
Endevco 2226	± 5% 2 cps–5 kc	25	±2% 0–1000 g	+3% −2% 200 cps–10 kc	Solar-panel tip

[a]With 1000–MΩ load.
[b]Term taken from vendor literature.
[c]Data evaluated to 10 kc. See Appendix for details.
[d]Three-hole, data from three-point mounting Columbia 514 tx (Z axis).
[e]Also type approval (TA) assembly.

III. INSTRUMENTATION

It is a foregone conclusion that results from any dynamic test are only as reliable as the instrumentation utilized to obtain the data. It is for this reason that the decision was made to test the accelerometer limitations of the data analyzed in this Report. In general, the results of the accelerometer test, included in Table 2, have demonstrated the adequacy of the instrumentation.

The test is described in detail in the Appendix. It consisted principally of analyzing the data from a reference standard accelerometer mounted back-to-back with the accelerometer to be calibrated. The same analysis parameters were utilized with this test as with the spacecraft environmental test analyses, to insure the same type of comparison.

Other equipment in the data channels can be considered flat to 10 kc. These include the tape recorders and amplifiers in the channels.

Endevco model 2217 accelerometers were used in the actual flight measurements of both *Ranger* and *Mariner-Mars*. The remainder of the flight telemetry consisted of a standard Inter-Range Instrumentation Group (IRIG) package mounted in the *Agena* second-stage vehicle. Present analysis techniques can limit the frequency response of such a system to the standard bandwidth frequency for the particular channel involved. However, as a result of the end-to-end calibration performed on the *Ranger VIII* and *IX* systems, it seems reasonable to extend the cut-off frequency of the channels to twice the nominal IRIG values without introducing a significant decrease in the signal-to-noise ratio.

The extended frequency range does limit the frequency response to 2000 cps. This is a small fraction of the possible response of test instrumentation.

In order to compare flight to test data at the present time, the test data must be modified by low-pass filtering at approximately twice the IRIG cut-off frequency. Extending the IRIG limits using an inverse frequency response analysis may be possible in the future. (In Fig. 8a, the *Mariner-Mars* PTM data have been low-passed at 2000 cps, utilizing a digital filter and are thus comparable with the Channel 17 flight data at twice IRIG; both of these measurements were taken at the same location on the internal section of Leg B, Fig. 6.)

The most significant flight pyrotechnic event seems to be the mechanical separation of the spacecraft. This event was lost on both *Ranger* and *Mariner-Mars* due to a channel switch-over to another monitoring instrument just before the separation took place. This would have been useful in defining the maximum pyrotechnic shock environment.

IV. ANALYSIS TECHNIQUES

A. Shock Spectrum Program

Pyrotechnic transients are, in general, so highly unstationary that no statistical methods of analysis are applicable. Also, an attempt to analyze these types of shock in the time domain would be of little value. Interpretation of these data in the frequency domain requires the use of a type of analysis such as shock spectra.

A digital program (JPL 5352) has been used to compute the spectra included in this Report.

The maximum response of a tuned simple resonator, excited by the transient, defines a single ordinate at one tuned frequency (abscissa) of a shock spectrum. By varying the tuned frequency of the resonator and plotting the *peak response* for each frequency, the shock spectrum is generated. The resulting plot is a specific type of frequency content of the transient pulse input. The units of the ordinate are peak g's response, while the abscissa is plotted as tuned frequency in cps. Another parameter associated with each spectrum is the *zeta* or percent of critical damping of the resonator which has the effect of smoothing the spectrum.

The IBM 7094 program computes the shock spectrum by solving the differential equation of motion of a simple resonator due to the applied transient and detecting the

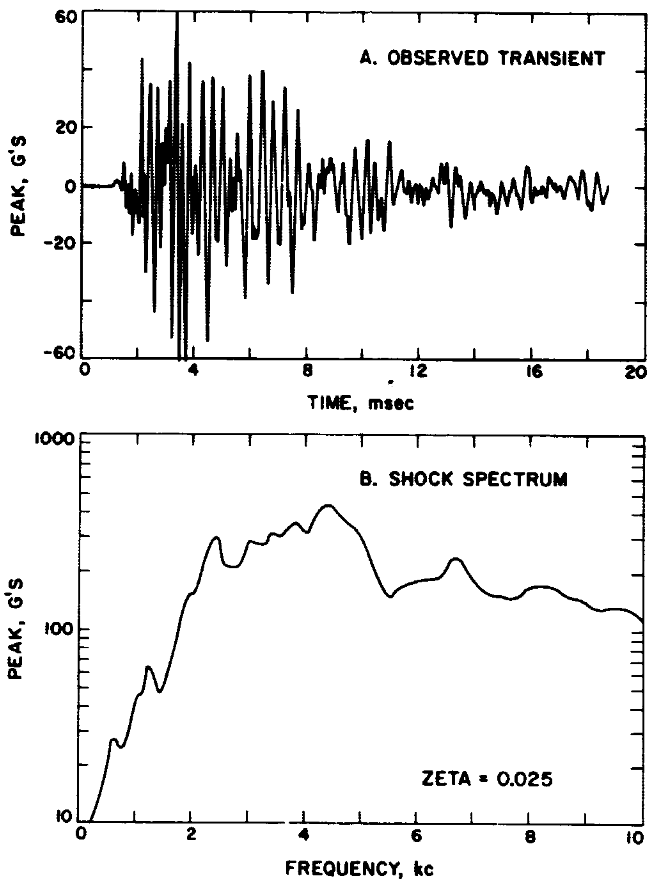

Fig. 7. Typical data analysis output, *Ranger* mechanical separation test at flight location

peak response. Eulerian numerical integration techniques are utilized in the solution of the equation. A Stromberg-Carlson 4020 plotter produces the output including the observed transient and the shock spectra associated with that transient. Various *zeta* values are usually used with each analysis, resulting in more than one shock spectrum for each transient. Included here are the spectra for 2.5% damping only. Typical data analysis output is shown in Fig. 7.

B. Spectra Manipulation Program

An advantage of digital processing is the convenient format of the output which lends itself to further comparison and compression of the data. The shock spectrum program has an output of punched IBM cards of the frequency spectra. Supplementary calculations can be performed using these cards as input data to an IBM 7094 computer.

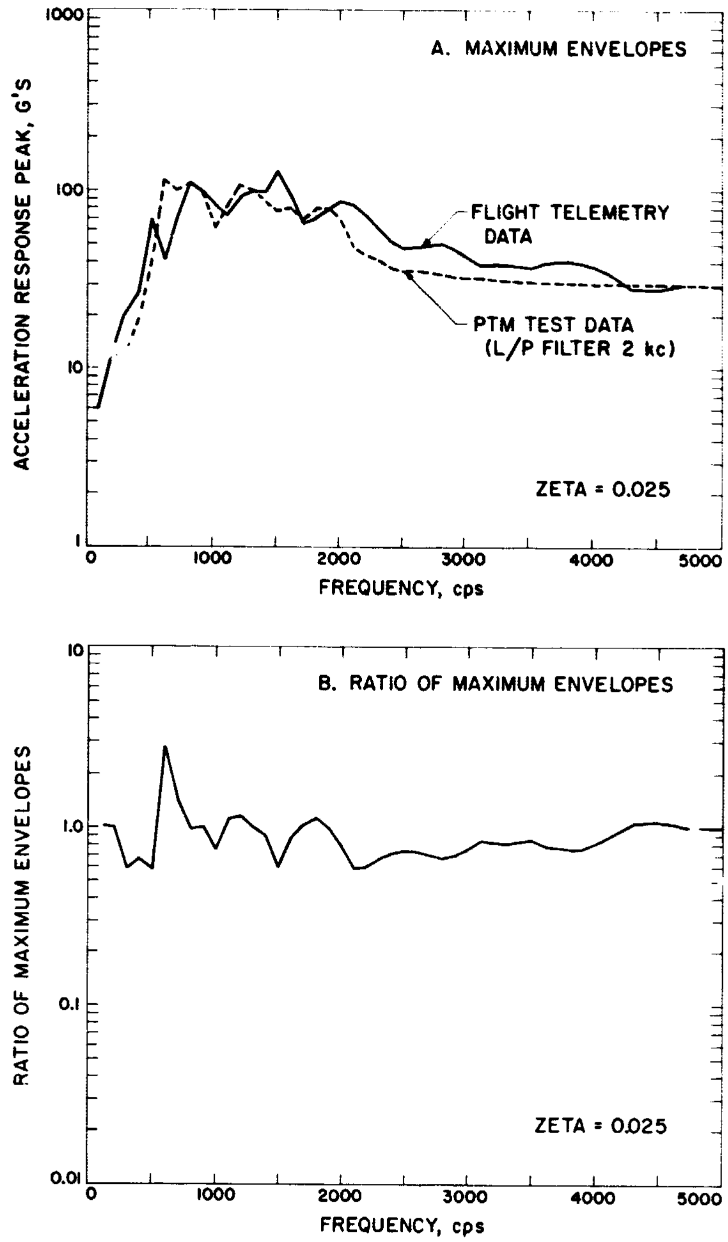

Fig. 8. Typical data manipulation examples, shock spectra of *Mariner-Mars* shroud-separation event

The JPL program 5574 can be utilized for comparison and manipulation of these data. There are seven manipulation operations available in the program as follows: mean, percentile levels (normal), percentile levels (log-normal), maximum envelope, minimum envelope, product, and ratio. Output data of this program are either IBM cards or SC 4020 plots, or both. Typical examples of the output of this program are shown in Fig. 8.

V. TEST DATA

Several comparisons using flight data, spacecraft test data, and assembly test data have been made.

The shock spectra for the *Ranger VIII* and *IX* shroud separation event and the ground tests of the mechanical separation on the PTM are compared in Fig. 9. The filtering effect of the telemetry system is apparent in the flight curve. The mechanical separation data could be filtered using a digital filter and a comparison made to the flight data as they are. But this would limit the data to a 2000-cps frequency range. The data were recorded from the accelerometer near Case IV shown in Fig. 10.

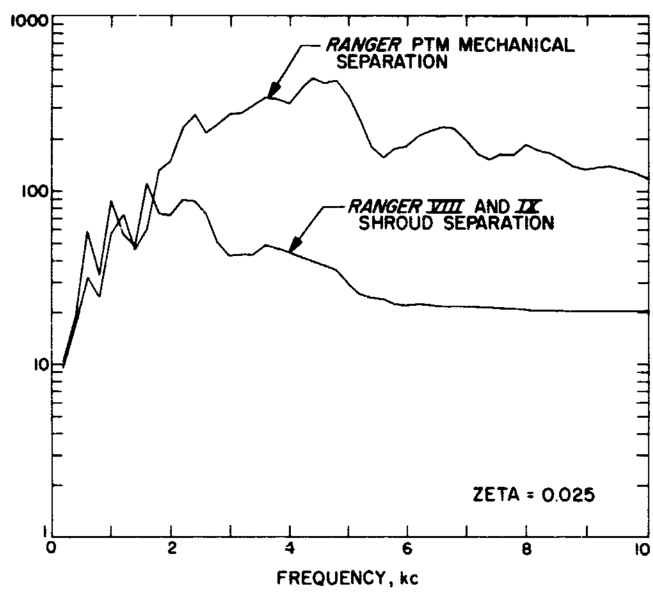

Fig. 9. Maximum envelopes of shock spectra, *Ranger* flight shroud separation, and PTM mechanical separation test

The *Ranger* bus response to the mechanical separation transient is given in Fig. 11. Several accelerometer locations in and on electronic Case IV were used. The sensitive axis was the spacecraft *X* axis. The PTM and *Ranger VI* were the test vehicles for these data. Thirteen data samples from five separate runs were used to compute the maximum-minimum envelope and the 95 and 50 percentile levels (assuming a normal distribution). It is interesting to note that the maximum envelope and the 95 percentile level are comparable. Figure 11 shows the amount of dispersion in the response that equipment would see when exposed to a severe pyrotechnic environment. A necessity for repeated firings is indicated; i.e., the statistical variations associated with pyrotechnic devices cause a variation in the response experienced by the test hardware. To increase the probability that a flight shock would be within the test limits, a series of repeated runs should be performed. Assuming a "*t*" distribution and small sample size, four or five runs would give significant results. Another possible method would be to increase the charge of the pyrotechnic, i.e., use a larger squib, for the environmental tests using live pyrotechnics.

In Fig. 12, the maximum envelope described above is compared to the maximum envelope from the TA shock test of the Case IV assembly which utilized the shock machine in Fig. 5. Three accelerometers (Endevco 2225) at various locations in the assembly were used as inputs. The test configuration and accelerometer locations are shown in Fig. 13. The transducers are sensitive in the spacecraft *X* axis. All the data from the five TA runs in the *X* axis were used in the analyses. Figure 12 shows that TA shock does not adequately cover the mechanical-separation shock at the higher frequencies. The TA shock does, however, cover the solar-panel deployment shocks at the high frequencies, as shown in Fig. 14.

The idealized TA shock spectrum would be one that would bracket the shock spectra of the mechanical separation event. However, this is not within the "state of the art" of present-day shock machines.

The responses to different events as measured at the interior center web of Case IV on the *Ranger* PTM is shown in Fig. 15a, b, c. The three events are electrical separation, mechanical separation, and solar-panel deployment. Each figure gives the 5 and 95 percentile levels. The data show that the mechanical separation produces the highest response. The same general trend can be noted in all the spectra, i.e., the highest response is at the higher frequencies, even though the different pyrotechnics are located at several locations on the spacecraft. The results would indicate that for ground testing of spacecraft systems, the minimal requirement would be the mechanical separation test. The solar-panel deployment has considerable dispersion at the high frequencies, resulting in a low confidence level in this portion of the spectra.

Figure 16 compares the shock spectra of a mechanical separation as seen at different locations on the spacecraft. The spacecraft Foot A response is very high because it is located directly above a pinpuller, as shown in Fig. 2. The Case I Leg A location is directly above the Foot location. The solar-panel-location shock spectrum is different

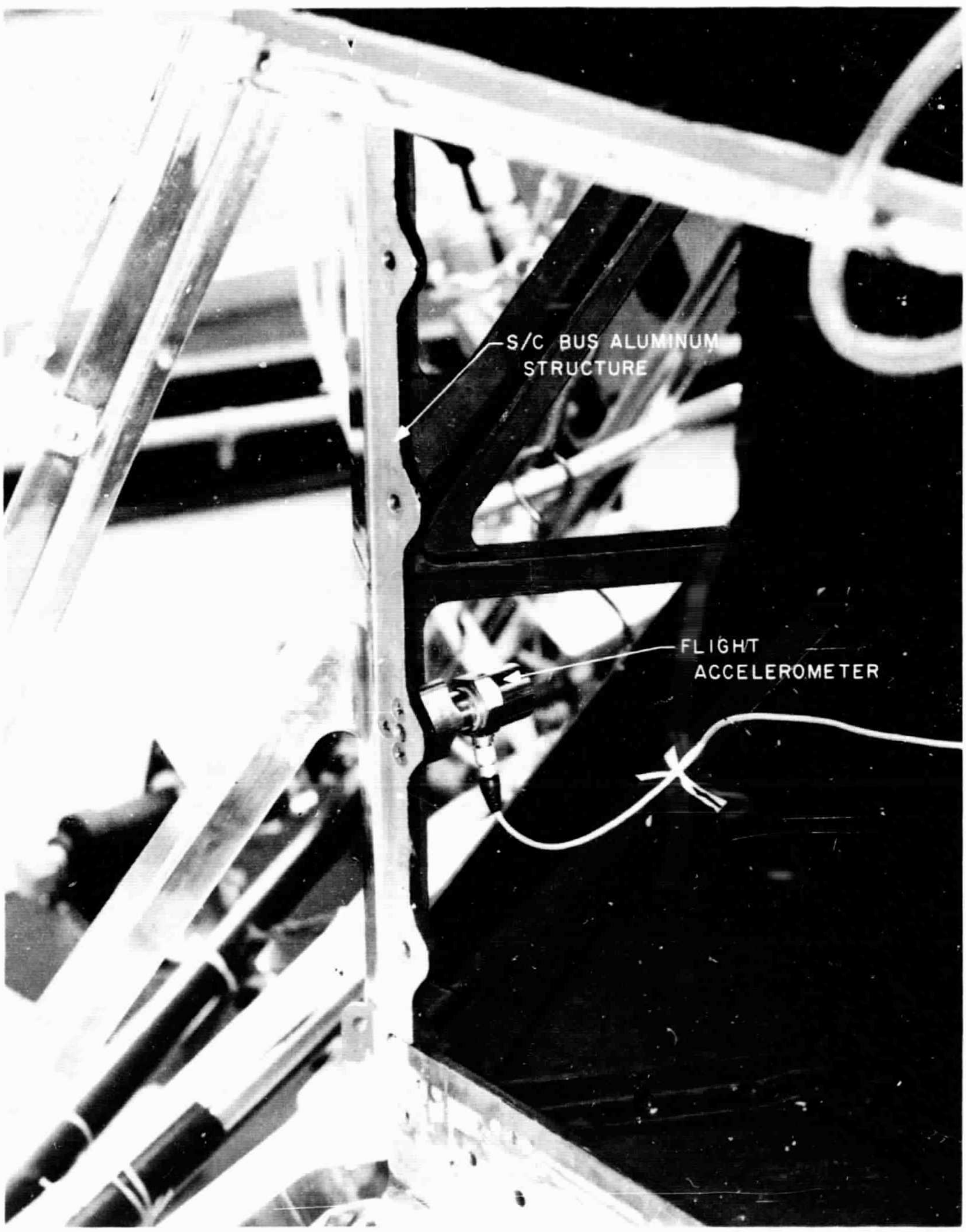

Fig. 10. Flight location of accelerometer on *Ranger VIII, IX* spacecraft bus (Case IV) removed

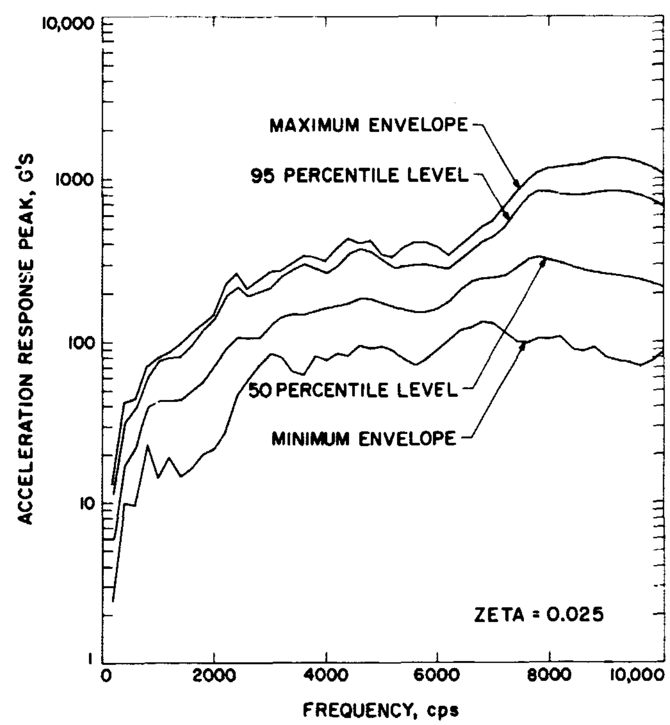

Fig. 11. *Ranger* Case IV response to mechanical separation

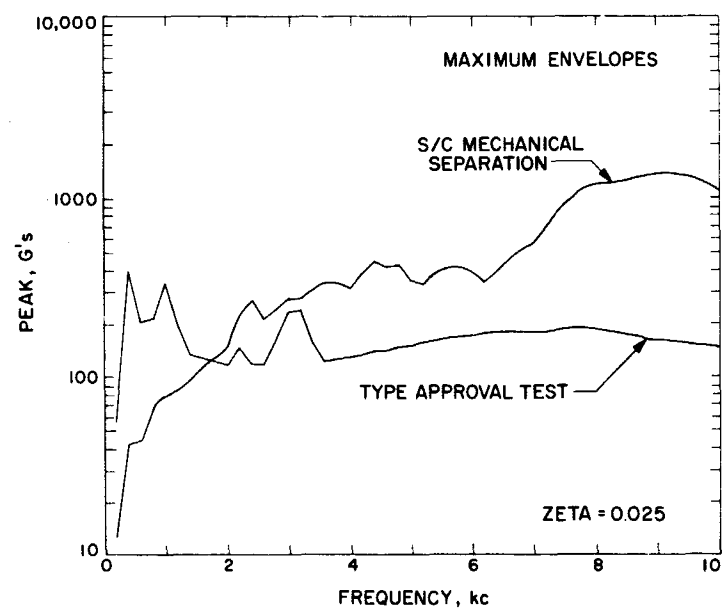

Fig. 12. Maximum envelopes of shock spectra, *Ranger* Case IV TA assembly shock, and spacecraft mechanical separation test

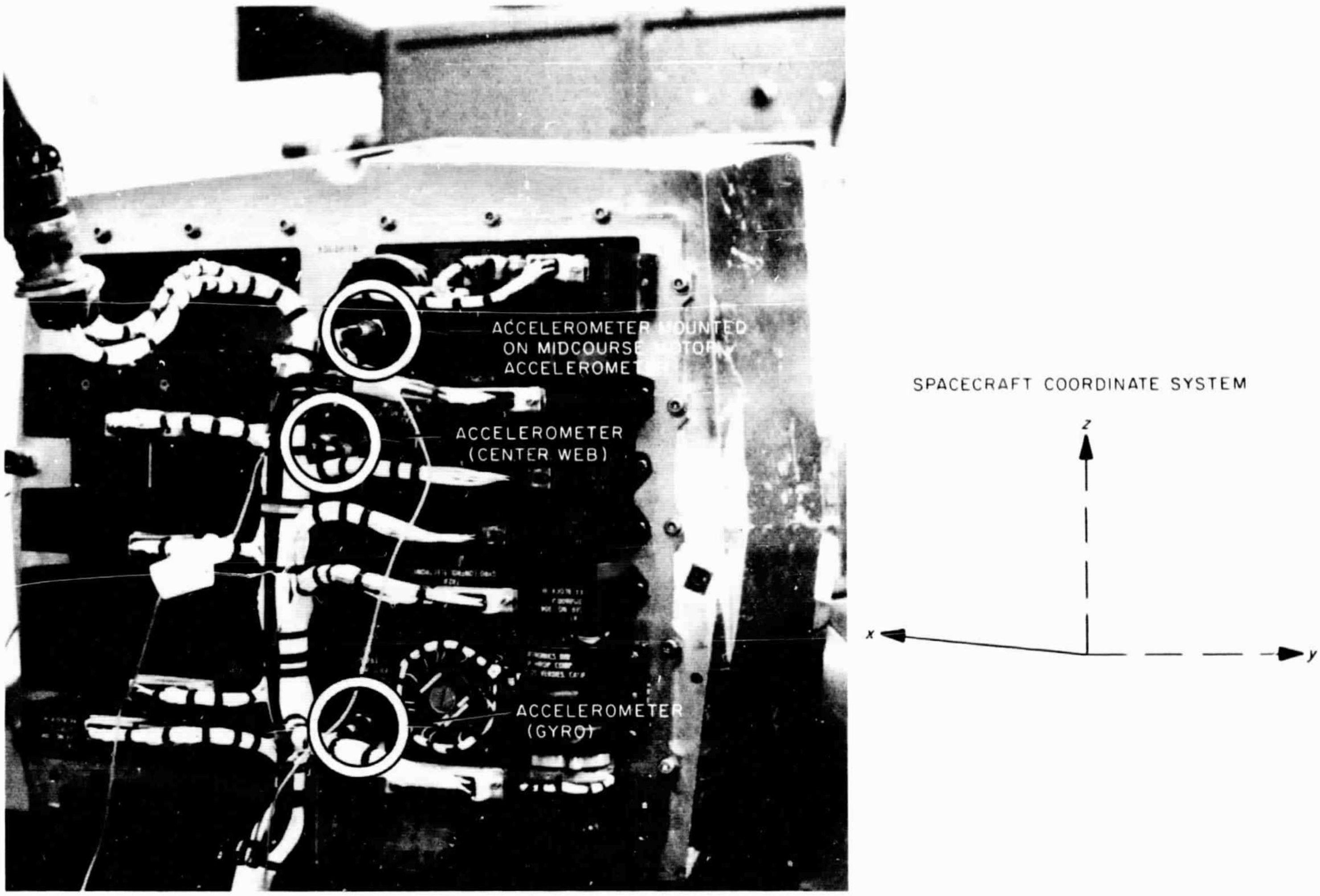

Fig. 13. *Ranger* TA Case IV shock test configuration, spacecraft X axis

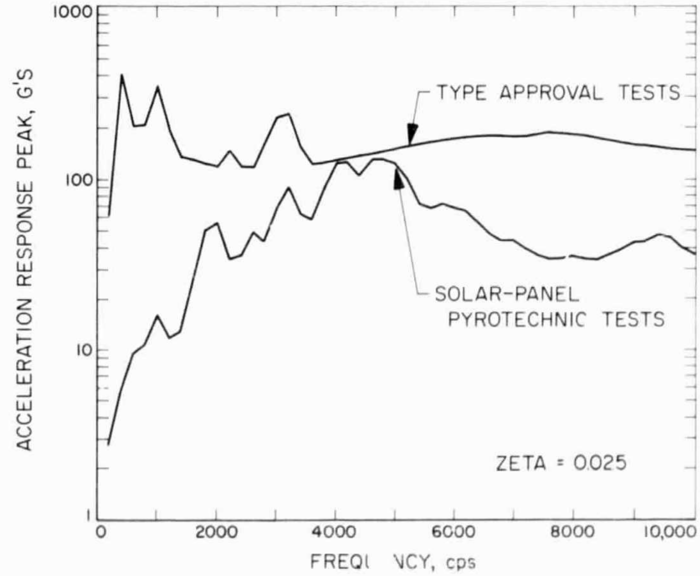

Fig. 14. Maximum envelopes of shock spectra, *Ranger* Case IV TA assembly shock, and spacecraft solar-panel deployment test

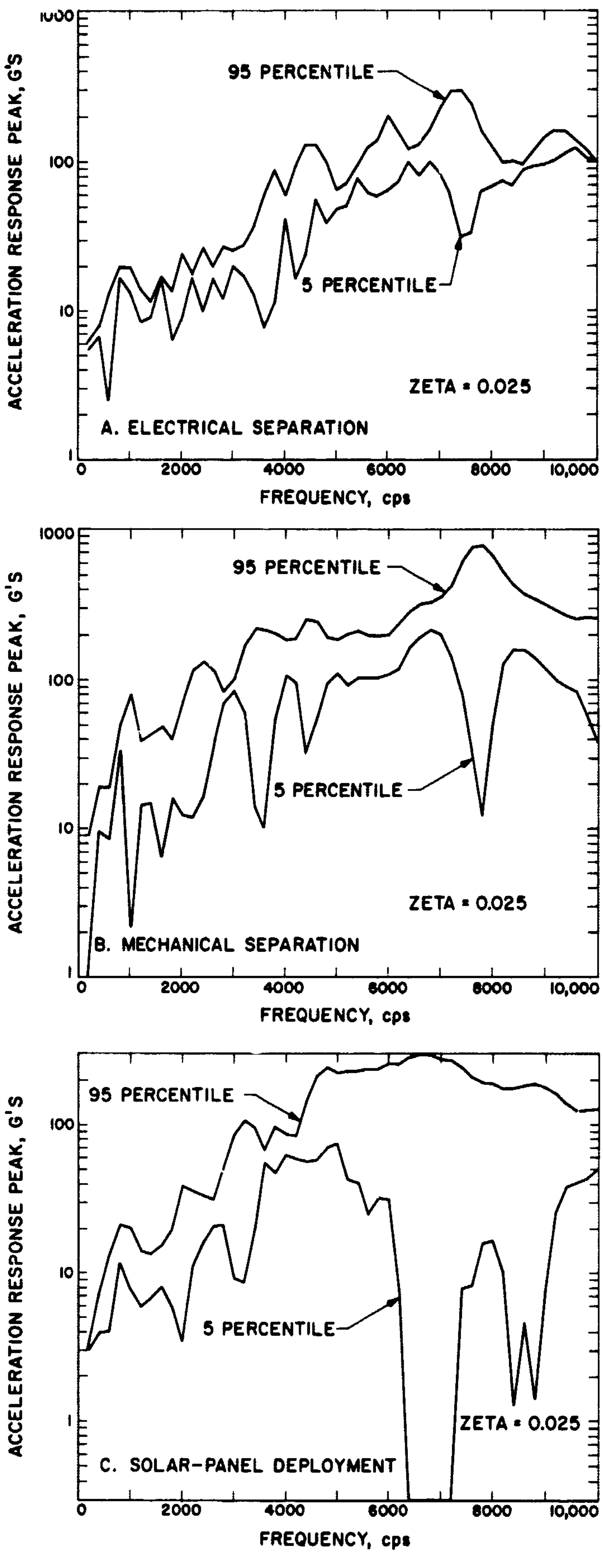

Fig. 15. Shock spectra, *Ranger* Case IV center web

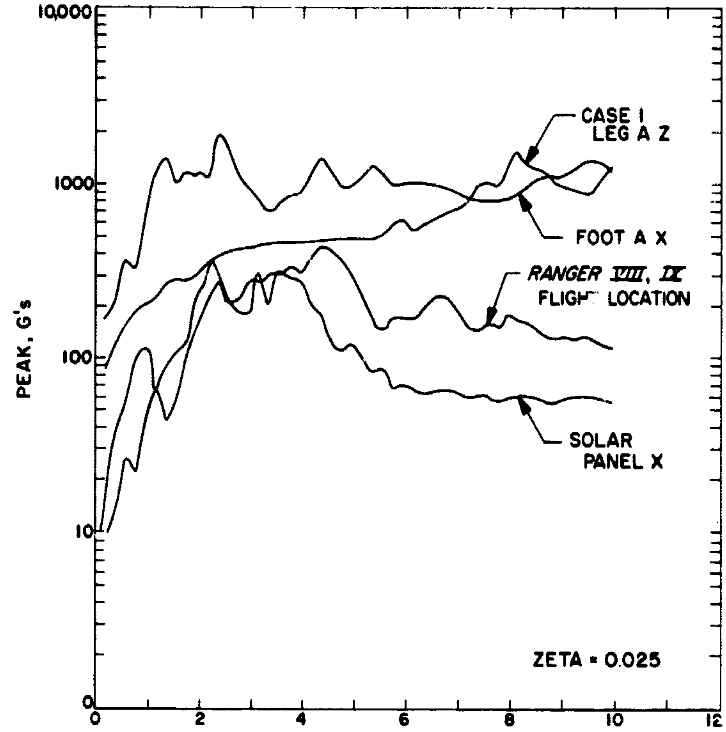

Fig. 16. Shock spectra, *Ranger* mechanical separation test

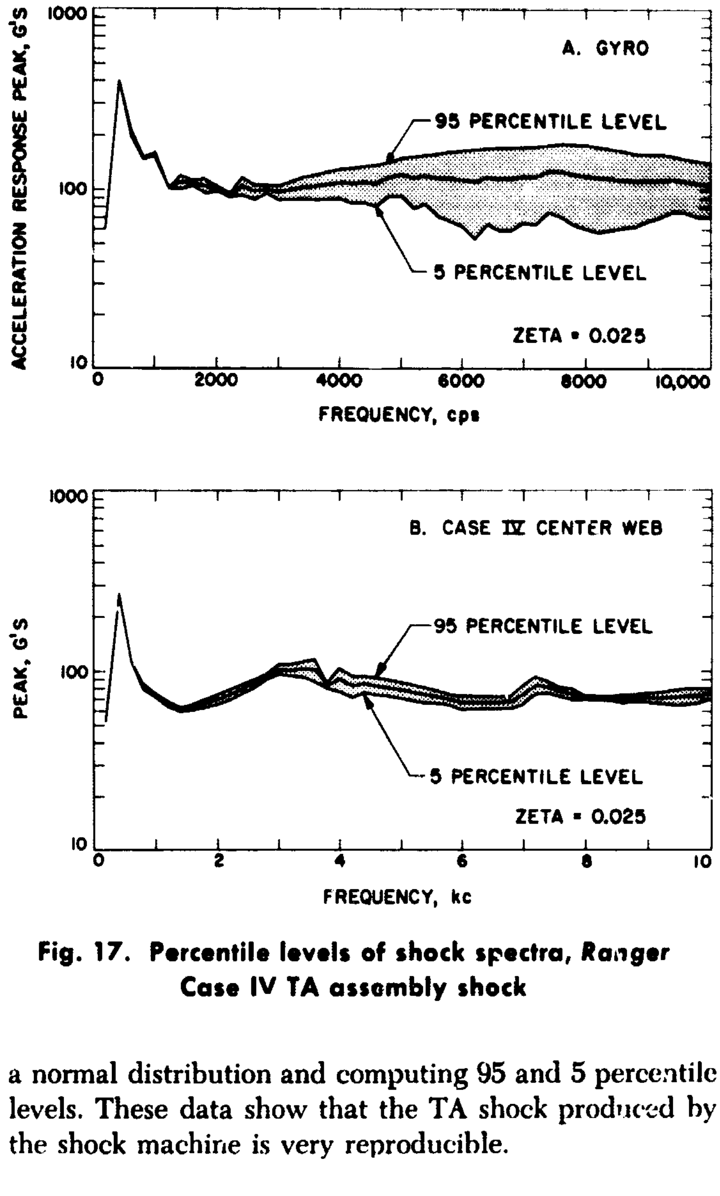

Fig. 17. Percentile levels of shock spectra, *Ranger* Case IV TA assembly shock

from other shock spectra, as could be anticipated because of the structural differences. These curves show that responses at different locations during the same test are widely scattered. This well-known result is emphasized to demonstrate the necessity for pyrotechnic tests at the system level. It would be very difficult to design an assembly level test that matches all of the spectra or even covers them adequately. If a test were specified to bracket adequately all the responses, then based on present shock machine capability, severe damage would occur due to the low-frequency content characteristic of shock test machines.

The reproducibility of the TA shock is demonstrated in Fig. 17a, b. Five consecutive shocks measured at the gyroscope location and at the midcourse-guidance accelerometer location shown in Fig. 13 were used in the plot. The envelope shown is the percentile envelope using a normal distribution and computing 95 and 5 percentile levels. These data show that the TA shock produced by the shock machine is very reproducible.

The maximum-minimum envelopes of the solar-panel shock at several locations on the *Ranger* spacecraft show that the responses are dispersed (Fig. 18a, b, c). This is typical of pyrotechnic data. Seven separate tests were used to compute the envelope indicated at each location. Consequently, the results are statistically significant and give an indication of the amount of variation that could be expected from several repetitions of the same test on different vehicles. The vehicles used were *Rangers* PTM, *VI*, *VII*, *VIII*, and *IX*.

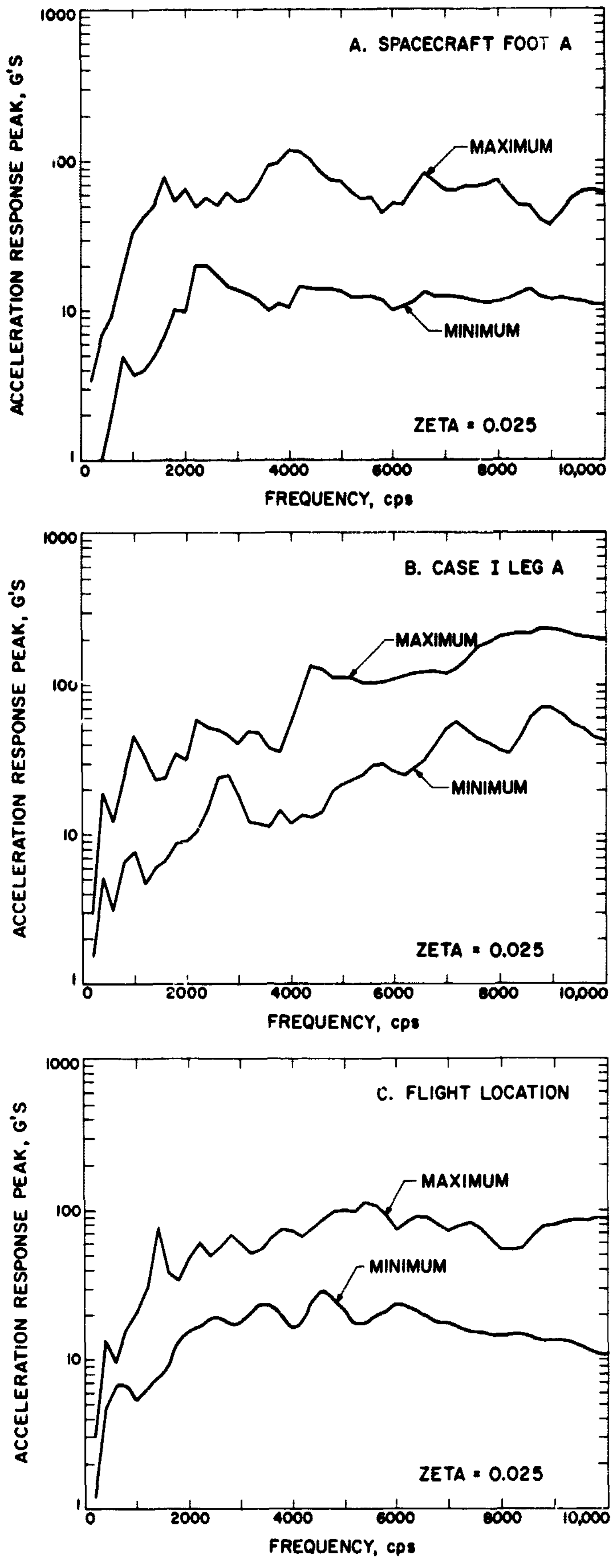

Fig. 18. Maximum and minimum envelopes of shock spectra, Ranger solar-panel deployment

VI. CONCLUSIONS

Extensive pyrotechnic shock measurements have been obtained from the ground testing of the *Ranger* and *Mariner-Mars* spacecraft using the actual explosive devices in their flight configuration.

The analysis of the data using shock spectra and statistical techniques has shown the following:

1. The mechanical separation shock is generally the most severe pyrotechnic shock experienced by the spacecraft. The response to the solar-panel pinpuller shock is reduced by the rubber grommets inserted between the pinpuller and the spacecraft. There is reason to believe, based on flight data from vehicle staging and shroud separation, that the shroud separation pyrotechnic is more severe in amplitude at the spacecraft flight location than the staging transients. The shock spectra from flight data, which are meaningful up to 2 kc, tend to support this. The shroud separation (on *Ranger*) was comparable to the mechanical separation shock although a direct comparison of flight data could not be made, because of telemetry problems.
2. The flight telemetered data are inadequate for shock measurement because of the lack of high-frequency response and absence of measurements of spacecraft separation.
3. Although results from the shock machine were highly reproducible, the responses did not cover those from pyrotechnic tests. Repeated firings, four or five, of the pyrotechnics on at least PTM-type spacecraft will demonstrate the reliability of the spacecraft in the environment. Although no system level failures have occurred during either the *Ranger* or *Mariner-Mars* test programs, there is no indication that the environment should be ignored.
4. The responses at the same location for different pyrotechnic devices (as used on the *Ranger*) tend to give the same spectra shape. Specifically, the highest response always occurs at a high frequency.

APPENDIX

Accelerometer Characteristics Under Transient Conditions

A special test was performed to determine the frequency response of typical accelerometers used for measurement of pyrotechnic shock data under a shock environment. The accelerometers are normally calibrated using a sinusoidal input. The response to transient excitation above 4 or 5 kc was not known.

A cylindrical projectile with a hemispherical end was dropped 12 in. onto a lead target ¼ in. × 1 in. × 1 in. The test accelerometer was mounted on top of the projectile.

The standard accelerometer, a Kistler standard directly traceable to NBS, was mounted in the interior cavity of the mounting block. The accelerometers were mounted back to back in the mounting block with a single stud except for the Columbia 514 and Endevco 2226. The Columbia 514 has a three-hole mount. The Endevco 2226 was attached with dental cement.

The projectile was suspended by an electromagnet. Data were recorded at 60 in./sec on an Ampex 1300 double-band tape recorder. The five accelerometers used are given in Table 2 of this Report. Each accelerometer was tested five times.

The height of the drop was determined by the objective of achieving approximately a 500-g shock.

The data were digitized at 160,000 samples/sec and played through the shock program. The frequency response up to 10 kc, as determined by comparing all accelerometers to the Kistler standard Model 808K2, is also given in Table 2.